

Characterization of Autocatalytic Conversion of Precursor BACE1 by Heteronuclear NMR Spectroscopy

Yu-Sen Wang,^{*,‡} Brian M. Beyer,[‡] Mary M. Senior, and Daniel F. Wyss

Schering-Plough Research Institute, 2015 Galloping Hill Road, Kenilworth, New Jersey 07033

Received June 1, 2005; Revised Manuscript Received October 19, 2005

ABSTRACT: Accumulation of the cytotoxic 40- to 42-residue β -amyloid peptide represents the primary pathological process in Alzheimer's disease (AD). BACE1 (β -site APP cleaving enzyme 1) is responsible for the initial required step in the neuronal amyloidogenic processing of β -amyloid precursor protein and is a major drug target for the therapeutic intervention of AD. In the present study, BACE1 is initially synthesized as an immature precursor protein containing part of the pre domain and the entire pro domain, and undergoes autocatalytic conversion to yield the well-folded mature BACE1 enzyme. To understand the mechanism of the conversion and the role of the pro domain, we monitored the autocatalytic conversion of BACE1 by heteronuclear NMR spectroscopy and used chemical shift perturbations as a probe to study the structural changes accompanying the autocatalytic conversion. NMR data revealed local conformational changes from a partially disordered to a well-folded conformation associated with the conversion. The conformational changes are largely concentrated in the NH_2 -terminal lobe. Conversely, the active site conformations are conserved during the autocatalytic conversion. The precursor and mature BACE1 proteins were further characterized for their ability to interact with a substrate-based transition state BACE1 peptide inhibitor. The precursor BACE1 rapidly adopted the bound conformation in the presence of the inhibitor, which is identical to the bound conformation of the mature protein. The interaction of the inhibitor with both the precursor BACE1 and the fully processed BACE1 is in slow exchange on the NMR time scale, indicating a tight binding interaction. Overall, the NMR data demonstrated that the pro domain does not hinder inhibitor binding and may assist in the proper folding of the protein. The fully processed BACE1 represents a high quality well-folded protein which is highly stable over a long period of time, and is suitable for evaluation of inhibitor binding by NMR for drug intervention.

Alzheimer's disease (AD)¹ is characterized by severe memory loss and neuronal cell death. Accumulation of the cytotoxic 40- to 42-residue β -amyloid peptide ($\text{A}\beta$) represents the primary pathological process in AD. Elucidating the molecular pathway involved in the generation of $\text{A}\beta$ is the key for rational therapeutic approaches to lower $\text{A}\beta$ concentration in AD. The $\text{A}\beta$ peptide is generated by endoproteolysis of the large type I membrane protein called the β -amyloid precursor protein (APP). APP is processed by three types of protease activities: α -secretase (1), β -secretase (2), and γ -secretase (3), the molecular identities of which were only identified in recent years. The β -secretase was identified as a novel membrane-associated aspartic protease, β -site APP cleaving enzyme 1 (BACE1) (2). Results from BACE1 knockout mice suggested that BACE1 is dispensable for normal development and physiological

functions in vivo. BACE1 is responsible for the initial required step in the neuronal amyloidogenic processing of APP and is a major drug target for the therapeutic intervention of AD.

The human BACE1 protein contains 501 amino acids (4), with an N-terminal signal pre-peptide (residue 1–21) followed by a pro domain spanning amino acids 22–45, which are removed post-translationally. Figure 1 shows a schematic representation of the protein domain structure of BACE1 (5). The protease domain extends from residues 46 to 460. BACE1 has a single predicted transmembrane domain of 17 amino acids (residues 461–477) and a short cytosolic domain of 24 amino acids (residues 478–501). Two aspartic protease active site motifs with sequences DTGS (residues 93–96) and DSGT (residues 289–292) are present on the luminal side of the membrane. Based on its amino acid sequence, BACE1 is predicted to be a type I transmembrane protein with the active site located on the luminal side of the membrane where β -secretase cleaves APP.

The crystal structure of the protease domain of human BACE1 in complex with a transition-state inhibitor referred to as OM99-2 has been determined recently to 1.9 Å resolution (6). OM99-2 is based on an octapeptide sequence of Glu-Val-Asn-Leu-Ala-Ala-Glu-Phe in which the Leu–Ala bond is substituted with a hydroxyethylene transition-state isostere. The K_i and K_d values of OM99-2 for

* To whom correspondence should be addressed. Phone: (908) 740-3402. Fax: (908) 740-4042. E-mail: allen.yu-sen.wang@spcorp.com.

[‡] These two authors contributed equally to this work.

¹ Abbreviations: $\text{A}\beta$, β -amyloid peptide; AD, Alzheimer's disease; APP, β -amyloid precursor protein; BACE1, β -site APP cleaving enzyme 1 (or β -secretase); preproBACE1, BACE1 containing part of the pre domain, the complete pro domain, and the protease domain (Ala14–Thr454); AutoBACE1, autocatalytically converted BACE1 with the pre and pro segments removed (Leu41– or Leu43–Thr454); HSQC, heteronuclear single-quantum correlation; NMR, nuclear magnetic resonance.

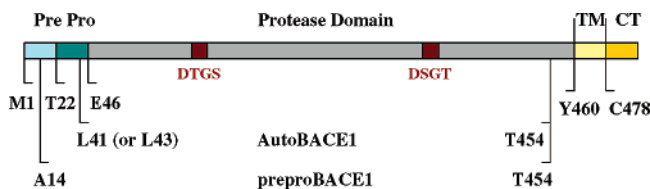


FIGURE 1: Schematic representation of the protein domain structure of BACE1 (5). BACE1 contains an aspartyl protease domain, pre and pro regions at the N-terminus, and a single transmembrane domain (TM) and a cytosolic tail (CT) near the C-terminus. DTGS and DSGT are the two active site motifs. The preproBACE1 used in this study contains the aspartyl protease domain, part of the pre domain, and the entire pro domain (Ala14–Thr454). AutoBACE1 is the autocatalytically converted aspartyl protease domain (Leu41–or Leu43–Thr454).

recombinant BACE1 protein have been determined to be in the low nM range (7). The BACE1 catalytic domain forms a typical bilobal structure that is similar to pepsin and other aspartic proteases despite their low sequence conservations. BACE1 shows less than 30% sequence identity with human pepsin family members. The inhibitor binds within the enzyme active site, engaging the active site aspartic acid residues. The two conserved aspartic acids in the active site are partially covered by a hairpin loop, also known as the “flap”. The “flap” is considered dynamic and important for protein–inhibitor interactions (6, 8). Substantial efforts have been made to develop active site-directed inhibitors of BACE1 (9–12).

All mammalian aspartic proteases are commonly synthesized as precursor proteins with a pro domain and are subsequently converted to active proteases. During the maturation process, the pro region is cleaved by diverse mechanisms. A typical function of the pro region in aspartyl proteases is to sterically block the active site, thereby preventing binding of substrate (13). In addition, the pro segments are frequently important for the folding, stability, and/or intracellular sorting of the precursor protein (14). BACE1 expressed in mammalian cells was derived from proteolytic processing at the junction between the putative pro and protease domains (5, 15). These observations suggest that the activation of BACE1 *in vivo* is likely mediated by another protease. It was recently reported that recombinant pro-memapsin 2 (pro- β -secretase or proBACE1) hydrolyzes peptide substrates at pH 4.0 but does not autocatalytically cleave within the pro region (7). Pro-memapsin 2 was activated *in vitro* by several proteases with trypsin-like specificity. The activity of pro-memapsin 2 stems from a part-time and reversible uncovering of its active site by its pro region. The cleavage of pro-peptide yielded permanently active memapsin 2. Another study of a soluble BACE derivative, ProBACE460, truncated between the protease and transmembrane domains, showed that the pro domain of proBACE460 does not suppress activity as in a strict zymogen, but does appear to facilitate the proper folding of an active protease domain (16). ProBACE460 was activated to mature BACE460 by treatment with furin.

In this study, we present a novel mechanism for BACE1 activation, an autocatalytic conversion of precursor BACE1 *in vitro*. BACE1 is initially synthesized as an immature precursor protein containing part of the pre domain and the entire pro domain, and subsequently undergoes an autocatalytic conversion to yield the activated mature BACE1

enzyme. To understand the mechanism of the conversion and the role of the pro region on a structural basis, we monitored the autocatalytic conversion of BACE1 by heteronuclear NMR spectroscopy, and used chemical shift perturbations as a probe to study the structural changes accompanying the autocatalytic conversion. NMR data revealed local conformational changes from a partially disordered to a well-folded conformation in the NH_2 -terminal lobe associated with the conversion from the immature precursor protein into the mature enzyme. However, it was found that the active site conformations were conserved during the conversion. Both the precursor and matured forms of BACE1 were able to interact strongly with a substrate-based transition-state BACE1 peptide inhibitor in the same bound conformation.

EXPERIMENTAL PROCEDURES

Protein Expression and Purification. The full-length human BACE1 cDNA in pCDNA4/mycHisA was obtained from the University of Toronto. The BACE1 cDNA clone encoded for amino acids 1–454. The human BACE1 protein (residues 14–454) was subcloned into pET 11a at the *Nde*I restriction site as a precursor protein containing the pre, pro, and protease domains, hereafter referred to as preproBACE1. PreproBACE1 was overexpressed at 37 °C in BL21(DE3) for 3 h. Cells were grown in TB and induced with 1 mM IPTG at an OD of 1.5. After expression, cells were resuspended in TN buffer (50 mM Tris pH 7.5, 150 mM NaCl) at one-tenth the original expression volume containing 10,500 units of benzoase per liter. Cells were lysed under pressure and applied to an equal volume 27% sucrose cushion. Inclusion bodies (IB) were recovered by centrifugation at 11,500g for 30 min. IB were then resuspended in TN buffer and further purified by passing over an equal volume 27% sucrose cushion. This procedure was then conducted two more times using TNT buffer (50 mM Tris pH 7.5, 150 mM NaCl and 1% Triton X-100). IB were then washed with TE buffer (10 mM Tris pH 7.4, 1 mM EDTA) and resuspended in TE buffer at a concentration appropriate for refolding.

For refolding, IB were pelleted from TE suspension and solubilized in 50 mM CAPS pH 10.7, 50 mM β ME, and 8 M urea at a protein concentration of up to 10 mg/mL. Following incubation with agitation at room temperature for 30 min, the solubilization solution was rapidly diluted 100-fold into water at room temperature. The pH was immediately adjusted to 8.7, and the refolding mixture was further incubated with slow stirring at room temperature for 4 h. Reshuffling reagents, reduced and oxidized glutathione, were then added at concentrations 1.0 mM, 0.1 mM respectively in the presence of 1 mM L-cysteine. The final pH was then adjusted to 8.7 for incubation at 4 °C with slow stirring. Activity was then monitored for up to 4 weeks to obtain maximal activity for purification (usually two weeks). For purification, refolding solutions were concentrated 100 \times and the protein was purified to homogeneity using gel filtration chromatography (Superdex 200) in 75 mM K_2HPO_4 pH 7.5, 150 mM NaCl, 0.015% sodium azide.

Uniform ^{15}N -labeling of BACE1 was performed in ^{15}N labeled minimal medium using $^{15}\text{NH}_4\text{Cl}$ as a sole nitrogen source. The ^{15}N labeled BACE1 protein at a concentration of 0.1 M was exchanged into a pH 7.5 buffer containing 75

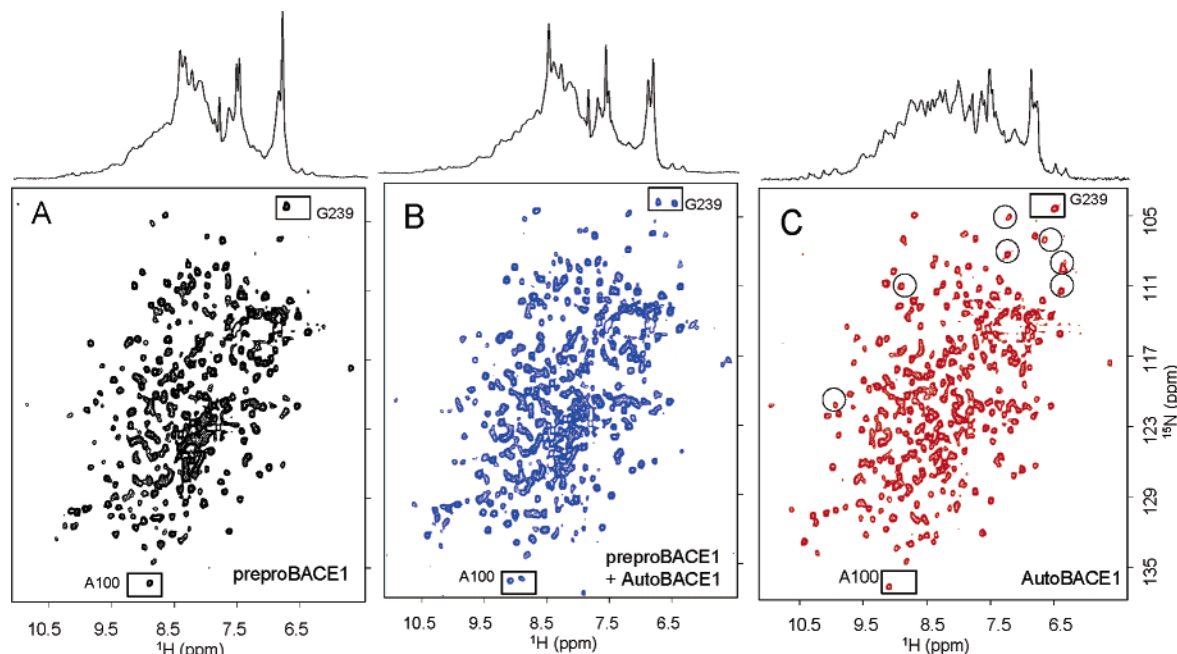


FIGURE 2: ^{15}N - ^1H NMR HSQC spectra of preproBACE1 protein immediately after sample preparation (A), after 64 h (B), and after 100 h (C) at 25 °C and pH 7.5. The 1D trace on top of each 2D spectrum is taken along the ^1H dimension. The inserted boxes show the chemical shift changes of residues Ala100 and Gly239, respectively. Circles in C indicate that some of the new peaks emerged at high and low frequency regions of the NMR spectrum of AutoBACE1. For clarity, the cleaved pre and pro peptides were removed from the NMR sample before the acquisition of the spectrum in C.

mM K_2HPO_4 , 150 mM NaCl, 0.015% sodium azide, and 5% D_2O for NMR studies. To study the autocatalytic conversion of BACE1, preproBACE1 was tested immediately after sample preparation by NMR. The BACE1 inhibitor, OM99-2, was purchased from Bachem Bioscience Inc. (King of Prussia, PA).

The pre and pro peptides of preproBACE1 were autocatalytically removed to yield the matured protease domain (AutoBACE1). N-Terminal sequencing of AutoBACE1 demonstrated that it is a 1:1 mixture of residues 41–454 and residues 43–454. Prior to N-terminal sequencing, samples were further purified using a Superdex 200 column pre-equilibrated in 75 mM K_2HPO_4 pH 7.5, 150 mM NaCl, 0.015% sodium azide to separate the cleaved protein and peptides.

NMR Spectroscopy. NMR experiments were performed at 25 °C on a Varian INOVA 600 MHz NMR spectrometer equipped with a 5 mM triple resonance probe head. The fast ^{15}N - ^1H NMR HSQC experiment was used to improve sensitivity and to avoid water saturation (17). All HSQC experiments were acquired with 96 scans per t_1 increment, 48 complex points, and a recycle time of 0.7 s. The spectral width was 8000 Hz with 1024 (t_2) complex points. Linear prediction to 96 complex points was performed in the indirect dimension before Fourier transformation. To study the autocatalytic conversion, each 2D HSQC spectrum of preproBACE1 was acquired immediately after sample preparation, and at 29, 36, 43, 50, 57, 64, 71, 78, 85, 101, 117, 125, and 150 h. After acquisition of the first HSQC data set, the NMR sample was kept at 5 °C during the first 29 h, and then at ambient room temperature for the remainder of the study. To evaluate inhibitor binding, 2D ^{15}N - ^1H NMR HSQC spectra were acquired for both preproBACE1 and AutoBACE1 before and after adding OM99-2. NMR data were processed and analyzed with Felix2000.1 (Accelrys, CA) on a Silicon Graphics workstation.

RESULTS AND DISCUSSION

Time Course To Reach Fully Processed BACE1. Figure 1 shows the domain structure of the BACE1 protein. The human BACE1 was expressed as a precursor protein containing the protease domain as well as part of the pre and the pro segments (Ala14–Thr454). During the autocatalytic conversion of preproBACE1, the pre and pro segments were removed, resulting in the mature AutoBACE1. We used heteronuclear NMR to monitor the progress of the autocatalytic conversion. To increase sensitivity and reduce NMR experimental time, the fast ^{15}N - ^1H NMR HSQC experiment was recorded with a short interscan delay. This sensitivity improved NMR experiment allowed a high quality 2D HSQC spectrum to be acquired for the 45 kDa protein in 2 h at a concentration of 100 μM . A series of ^{15}N - ^1H NMR correlated HSQC spectra were recorded at different time points after sample preparation to monitor protein changes during autocatalytic conversion. The time course to reach fully processed BACE1 was determined. Figure 2 shows 2D ^{15}N - ^1H NMR HSQC spectra of preproBACE1 recorded immediately after sample preparation, and at 64 and 100 h. As the autocatalytic conversion proceeded, a new set of cross-peaks emerged and the intensities of these peaks gradually increased with time, while the intensities of the original peaks from preproBACE1 were reduced. As shown in Figure 2B, many residues show two sets of resonances in the NMR spectrum, indicating the coexistence of two states of the protein. The new set of peaks corresponds to the fully processed AutoBACE1 and the other set of peaks to the unprocessed preproBACE1. After about 100 h (Figure 2C), the peaks from preproBACE1 were completely gone. On the other hand, the new peaks from the processed protein were intensified. The protein was fully converted to AutoBACE1.

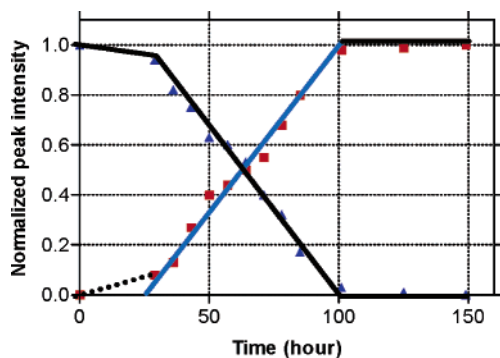


FIGURE 3: The peak intensity of Ala100 of preproBACE1 (blue triangles) and AutoBACE1 (red squares) as a function of processing time at 25 °C and pH 7.5, indicating that fully processed AutoBACE1 can be obtained within 3 days. The NMR sample was held at 5 °C between the acquisition of the first and the second data points. The true kinetics at 25 °C can be approximated by the solid blue line.

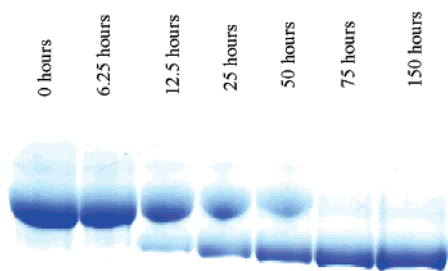


FIGURE 4: Time dependent conversion of preproBACE1 to AutoBACE1 as analyzed by SDS-PAGE. Protein was incubated at 5 mg/mL in 75 mM K_2HPO_4 , pH 7.5, 150 mM NaCl, 0.015% sodium azide, and 5% D_2O at 25 °C with 10 μg aliquots being removed and quenched (boiled) at the corresponding time points.

While the peak intensities of the unprocessed protein were rapidly reduced with time, the peak intensities of the autoprocessed protein were increased. Figure 3 shows the change in peak intensities for residue Ala100 as a function of time. At 100 h after sample preparation, the peak intensity reached a maximum with no further peak intensity changes observed after 100 h. Because the NMR sample was at 5 °C during the first 29 h and then at 25 °C for the remainder of the study, the true kinetics at 25 °C can be represented by the solid blue line. The time required for the conversion from the unprocessed protein to the autoprocessed protein at 25 °C is about 75 h.

Further evidence for the proteolytic cleavage is obtained from SDS-PAGE data. Figure 4 shows the time dependent conversion of preproBACE1 to AutoBACE1 as analyzed by SDS-PAGE. Protein was incubated at 5 mg/mL in the same buffer as that for NMR studies (75 mM K_2HPO_4 , 150 mM NaCl, 0.015% sodium azide and 5% D_2O) at 25 °C. A 10 μg aliquot was removed and quenched by boiling at the corresponding time point. The percentages of protein converted at the corresponding time points were the same as those shown in Figure 3. At 75 h, the preproBACE1 was fully converted to AutoBACE1. The SDS-PAGE data demonstrated time dependent conversion of preproBACE1 to AutoBACE1 that occurs with the same kinetics as the changes in NMR spectra. The apparent second-order rate constant for BACE1 autocatalytic conversion was calculated to be $0.05 \pm 0.01 \text{ mg}^{-1} \text{ min}^{-1}$.

It has been previously demonstrated that ProBACE460 has an activity profile that is virtually identical to that of fully processed BACE460 (16). This observation distinguishes BACE1 from the typical members of the aspartyl protease class. The same was observed in our studies. Therefore the kinetics for preproBACE1 and AutoBACE1 are the same.

Accelerated Autocatalytic Conversion. The fully processed protein from the NMR sample was subjected to amino-terminal sequencing. Amino-terminal sequencing indicated a 1 to 1 mixture of $\text{L}^{41}\text{RLPRE}$ to $\text{L}^{43}\text{PRETD}$. LC-MS analysis confirmed the amino-terminal sequencing data. Furthermore, total activity of the fully processed material was measured in the BACE1 functional assay (18). NMR data demonstrated that the autocatalytic conversion of BACE1 can be accelerated by exposure to ambient room temperature. A fully processed, well folded state can be reached within 3 days at approximately 25 °C at ~15 mg/mL concentration. In contrast, it requires 18 days at 4 °C in a conventional NMR sample preparation at a protein concentration of 5–10 mg/mL. The speedier processing due to higher temperature conditions can save about two weeks in sample preparation.

The cross-peaks of AutoBACE1 have distinct chemical shifts from those of the unprocessed protein. The exact extent of the processing can be estimated from the ratio of the peak intensities. It appears that NMR is a better method to evaluate the extent of processing than the usual methods using SDS-PAGE and sequencing data. In the study of BACE1, we used NMR to routinely monitor the extent of BACE1 autocatalytic conversion during protein preparation.

Autocatalytic Conversion of PreproBACE1. Many proteases are synthesized as inactive precursors to prevent unwanted protein degradation and to enable spatial and temporal regulation of proteolytic activity. During the maturation process, the catalytically active protease domain is released from the larger pro-enzyme. The mechanisms of conversion to active enzymes are diverse in nature, ranging from enzymatic or nonenzymatic cofactors that trigger activation, to a simple change in pH that results in conversion by an autocatalytic mechanism (13). The primary structure of BACE1 expressed in mammalian cells suggests that BACE1 is synthesized *in vivo* as proBACE1 and converted to mature BACE1 by an activating protease. It was shown that BACE1 expressed in human embryonic kidney 293T cells that were transfected with the full-length BACE cDNA had an N-terminal sequence that began at the protease domain (5). The full-length Asp2 (BACE1), which was expressed in Chinese hamster ovary cells, also demonstrated proteolytic processing at the junction between the pro and protease domains by N-terminal sequencing (15). Edman degradation of human brain BACE1 revealed an N-terminal amino acid sequence of that of the protease domain (19). In the study of proteolytic activation of recombinant pro-memapsin 2 (pro- β -secretase or BACE1), pro-memapsin 2 was activated *in vitro* by several proteases. It was observed that although recombinant pro-memapsin 2 hydrolyzed peptide substrate at pH 4.0, it does not autocatalytically cleave within its pro region (7). Recently, it was reported that the pro domain of proBACE460 does not confer zymogen-like properties but does assist in proper folding of the protease domain. The pro region of proBACE460 was cleaved by furin (16).

In this work, we presented an alternative mechanism for the activation of BACE1, the autocatalytic conversion of preproBACE1 *in vitro*. Incubation of preproBACE1 with the BACE1 inhibitor OM99-2 blocked the cleavage of the propeptide. Therefore, removal of the propeptide is specific to BACE1 and not due to small amounts of a contaminating protease. This observation confirms that the cleavage of preproBACE1 is autocatalytic. Figure 3 shows the time course of the autocatalytic conversion of preproBACE1 at 25 °C. The kinetics of autoconversion *in vitro* are slow because this is a totally different mechanism from the conversion of precursor BACE1 by other proteases *in vivo* and *in vitro*. At physiological temperature (37 °C), the conversion was accelerated but protein precipitation occurred *in vitro*, preventing NMR study at physiological temperature. For NMR study, 25 °C is a good balance between slower conversion (4 °C) and protein degradation (37 °C).

Well-Folded Conformation of AutoBACE1. In the 1D spectrum of preproBACE1 traced over the 2D HSQC spectrum (Figure 2A), the peak intensities are much higher, ranging from 7 to 9 ppm in the middle of the proton dimension as compared to that for the fully processed BACE1 (Figure 2C). In the 2D HSQC spectrum of preproBACE1 (Figure 2A), clustering of peaks in the central region of the amide spectrum indicates the presence of partial protein disorder. Many cross-peaks are weak or missing at high and low frequency regions (below 7 ppm and above 9 ppm, respectively). This observation is consistent with the appearance of the rather broad resonances in the 1D ^1H spectrum (Figure 2A), and indicates that part of the protein has substantial motional freedom (20). This disordered structure is due to (1) the unstructured pre and pro segments and (2) the partially disordered structure of the NH_2 -terminal lobe of the protein (see below). The unstructured pro segment is consistent with the observation that only the last six of the 21 residues in this segment were visible in the electron density map of the reported X-ray crystal structure of memapsin 2 (β -secretase or BACE1) complexed with the inhibitor, whereas the others were likely mobile, and thus not observed (6). This is also consistent with an unstructured pro segment being displaced from the active-site cleft by the inhibitor (7). By contrast, the cross-peaks from the fully processed BACE1 (Figure 2C) are typical of those of a highly structured protein. As the conversion progressed, the intensities of the peaks for preproBACE1 were gradually reduced and peak intensities from AutoBACE1 were increased. In addition, there are new peaks appearing at high and low frequency regions of the 2D NMR spectrum and the resonances become much sharper in the 1D proton spectrum (Figure 2C). The cross-peaks for AutoBACE1 are more evenly distributed along the proton as well as the nitrogen dimensions, indicating a well-defined solution conformation.

Conformational Rearrangement of BACE1 Autocatalytic Conversion. Near complete (>83%) assignments of the backbone resonances have been obtained for the catalytic domain of human BACE1 (21). The assigned backbone ^1H and ^{15}N chemical shifts of AutoBACE1 can be used as probes of structural changes accompanying the autocatalytic conversion process of BACE1 (22). The assignments of preproBACE1 are prohibitively difficult to accomplish for the following reasons. As described above, many cross-peaks are weak or missing at high and low frequency regions

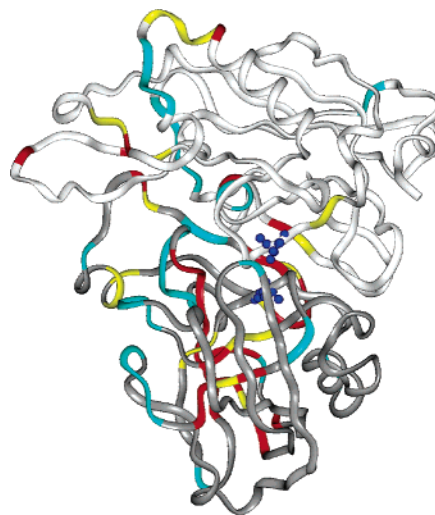


FIGURE 5: Chemical shift perturbations of BACE1 accompanying the autocatalytic conversion of BACE1. The backbone C^α trace of the crystal structure of free BACE1 (PDB entry: 1SGZ) is shown. Each residue is colored-coded according to its per residue weighted average chemical shift perturbation ($\text{WA} = [(\Delta\delta\{^1\text{H}\})^2 + (0.2 \Delta\delta\{^{15}\text{N}\})^2]^{1/2}$). Residues with $\text{WA} = 0.1\text{--}0.2$ ppm and > 0.2 ppm are shown in yellow and red, respectively. Residues with a $\text{WA} < 0.1$ ppm are dark gray and light gray for the NH_2 -terminal lobe (residues 49–241) and the COOH -terminal lobe (residues 242–454), respectively. The unassigned residues are shown in cyan. Two active site aspartic acids are shown in blue by using ball-and-stick models. The hairpin loop in front is the flap (Lys126–Glu140). The inhibitor binding site is located in the substrate binding cleft between the NH_2 - and the COOH -terminal lobes.

(below 7 ppm and above 9 ppm, respectively) in the 2D HSQC spectra of preproBACE1. Many peaks are clustered in the central region. As shown in the 1D ^1H spectrum (Figure 2A), the resonances of preproBACE1 are rather broad. In addition, the protein is constantly changing because of autoprocessing. However with the assignment of the fully processed BACE1, it is possible to follow the chemical shift changes accompanying the autoconversion by careful examination and comparison of all the HSQC spectra acquired at different time points. There are several types of changes that were tracked: (1) During the autoprocessing, many residues showed two peaks. By following the intensity changes of the two peaks, it can be determined with certainty that these two peaks belong to the same residue. Examples are shown in Figure 2B for Ala100 and Gly239. (2) Many peaks had weak intensities in the 2D HSQC of preproBACE1, but these intensities were increased gradually during autoprocessing. Obviously, the original weak peak from preproBACE1 and the intense peak of AutoBACE1 belong to the same residue. (3) The original peaks were missing for preproBACE1 but emerged during processing for AutoBACE1. By inspecting the HSQC spectra, the time course of the peak intensity changes can be followed. An example of this case is Gly74 shown in Figure 6. In this case, the original peak of Gly74 of preproBACE1 was not observed and the peak of Gly74 of AutoBACE1 was well defined. These peaks can then be classified as $\text{WA} > 0.2$ ppm in Figure 5. (4) Finally, many residues, especially those in the COOH -terminal lobe, experience small or no chemical shift changes.

Substantial chemical shift changes were observed for many residues in the NH_2 -terminal lobe (Figure 2), indicating local

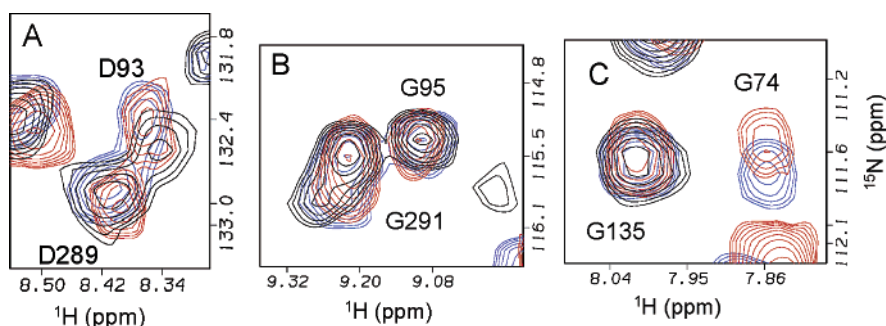


FIGURE 6: Active site conformations are conserved during the autocatalytic conversion of BACE1. Expanded region of the 2D ^{15}N – ^1H HSQC spectra of preproBACE1 protein immediately after sample preparation (black), after 64 h (blue), and after 100 h (red) for residues D93 and D289 (A), for residues G95 and G291 (B), and for residues G135 and G74 (C).

conformational changes during the conversion. It is unlikely that the observed chemical shift perturbations upon cleavage indicate the disappearance of the interaction between AutoBACE1 and the pro sequence for a number of reasons that are described next. In the 2D HSQC spectrum of preproBACE1, clustering of peaks in the central region of the amide spectrum indicates the presence of protein disorder which disappears upon cleavage of the pre and pro segments, suggesting that these segments are unstructured in preproBACE1. This observation is consistent with (1) the unstructured and mobile pro segment in the X-ray structure of BACE1 (6); (2) the finding that the pro domain has little effect on the active site (16); and (3) the observation that the overall distribution of cross-peaks in the 2D HSQC spectra of AutoBACE1 remained the same after removing the cleaved pre and pro peptides from the NMR sample. Another possibility is that these chemical shift changes may be caused by the interactions of parts of the prepro sequence with the protease domain of BACE1. In a model proposed on the basis of crystal structures from other mammalian aspartic protease zymogens, the conformation of the pro domain of pro-memapsin 2 (pro- β -secretase) exists in two equilibrium forms: one with the active site “open” and another one with the active site “closed”. In the closed form, the pro peptide assumes its native conformation and blocks the entrance of the active site cleft (7). If this model was correct, the interaction would cause chemical shift changes of residues within the active site, within both the NH_2 - and COOH -terminal lobes, and within the flap which partially cover the entrance of the active site. This is, however, inconsistent with the observed chemical shift changes that are largely concentrated in the NH_2 -terminal lobe, but occur neither in the COOH -terminal lobe nor in the active site. This is further inconsistent with the fact that the flap residues exhibited either no or only very small chemical shift changes. In yet another possibility the observed chemical shift changes could be caused by an interaction of parts of the prepro sequence with the NH_2 -terminal lobe. However, the mode of this interaction is not clear. The assumption for the interaction does not agree with the following observations: There are two types of cross-peaks for the same residue in the 2D HSQC spectra: well-defined peaks for both preproBACE1 and AutoBACE1, and very broad peaks for preproBACE1 which become narrower for AutoBACE1. If this was caused by an interaction between the prepro sequence and BACE1, the two types of peaks would indicate two different types of interactions on the NMR time scale: slow exchange and intermediate exchange, respectively. For the

interaction in intermediate exchange, the cross-peaks of the prepro sequence should be broadened. For the interaction in slow exchange on the NMR time scale, the bound prepro sequence should exhibit well-distributed cross-peaks. However, these are not consistent with much higher peak intensities in the central region of the 1D and 2D spectra of preproBACE1 (Figure 2A) and that all well-distributed cross-peaks in the 2D HSQC spectra belong to AutoBACE1. In addition, residues with chemical shift changes (Figure 5 below) in the NH_2 -terminal lobe do not form a well-defined binding site for the prepro sequence.

In Figure 5, the per residue weighted average chemical shift perturbations (WA) were color-coded onto the crystal structure of free BACE1 (8). The chemical shift changes due to conformational changes are spatially concentrated in the NH_2 -terminal lobe. Very large chemical shift changes were observed for residues in an eight-stranded β sheet A: Gln73 to Thr80 in strand 2, Ala100 to Ala103 in strand 5, and residues Leu145 to Thr155, which form part of the C-termini of strand 7 and the linker between strands 6 and 7. Very large chemical shift changes were observed also for all residues in strand 1 of a five-stranded β sheet C (Gly233–Ile237), residues Ser212 and Leu213 in strand 2, most residues of helix 6, and residues in the linker (Gly238 to Ile240) between strand 1 and helix 6. This is also the region at the NH_2 -terminal lobe side at the junction between the NH_2 - and the COOH -terminal lobes. NMR chemical shift perturbations revealed local conformational changes of the NH_2 -terminal lobe during the conversion. In contrast, only a few separated regions in the COOH -terminal lobe exhibited chemical shift changes. For example, the last four residues of helix 8 (Ala311 to Ser314) and the following linker (Thr315 to Glu316) to helix 9 displayed large chemical shift changes.

Active Site Conformations Conserved during Autocatalytic Conversion. In contrast to the large conformational changes described above, the active site residues experienced much smaller chemical shift changes during the autocatalytic conversion from preproBACE1 to AutoBACE1. BACE1 contains two aspartic protease active site motifs with sequences DTGS (residues 93–96) and DSGT (residues 289–292). The two active site aspartic acid residues (Asp93 and Asp289) showed only small chemical shift changes (WAs of Asp93 and Asp289 < 0.1 ppm) (Figure 6A); and other residues in these two active site motifs (Thr94, Gly95, Ser96, Gly291, and Thr292) displayed no or only very small chemical shift changes (WA < 0.1 ppm). Similarly, residues in the S1, S2, and S1' to S3' substrate binding pockets

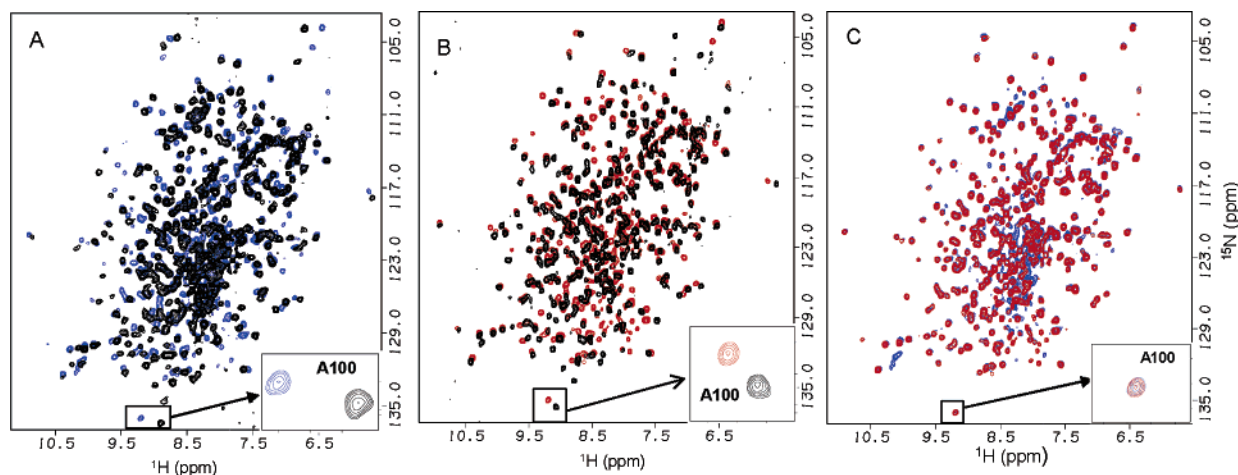


FIGURE 7: Interaction between BACE1 and inhibitor OM99-2. (A) 2D ^{15}N – ^1H NMR HSQC spectra of preproBACE1 in the absence (black) and presence of OM99-2 (blue). (B) 2D ^{15}N – ^1H NMR HSQC spectra of AutoBACE1 in the absence (black) and presence of OM99-2 (red). The inserted boxes show the chemical shift change of residue A100 upon inhibitor binding. (C) Overlay of the ^{15}N – ^1H NMR HSQC spectra of preproBACE1 (blue) and AutoBACE1 (red) in complex with OM99-2, showing that the bound conformations are nearly identical for both proteins.

experienced either no or only very small chemical shift changes. Figure 6B, for example, shows Gly291 in S1 and Gly95 in S1' experiencing very small and no chemical shift changes, respectively. The hairpin loop known as the "flap" is very flexible and plays an important role in the binding of inhibitors (8). Most residues of the flap region (from Lys126 to Glu140 with the exception of Thr133 which is not assigned) exhibited small chemical shift changes. A residue in the flap, Gly135, which is isolated from the crowded region in the HSQC spectrum, and thus can be used as a marker for the conformational change of the flap, showed no chemical shift changes (Figure 6C). In contrast to the active site regions described above, residues that form part of the S3 subpocket (Gln73, Gly74, and Lys75) and the following residues (Lys76 to Thr80) displayed very large chemical shift perturbations. However, these residues are at the N-termini close to the cleavage site within the pro region. For example, Figure 6C shows the cross-peak of Gly74, an S3 residue, in the HSQC spectra acquired at 64 and 100 h after sample preparation. Note that the cross-peak of Gly74 for preproBACE1 cannot be recognized, suggesting that it has very different ^{15}N – ^1H NMR chemical shifts in the two different forms of the protein. Taken as a whole, these NMR data demonstrated that the conformation of the active site is relatively well conserved while the protein undergoes local conformational changes in the NH_2 -terminal lobe during autocatalytic conversion yielding a well-folded structure.

Interaction with BACE1 Inhibitor. The X-ray crystallographic structure of memapsin 2 (β -secretase or BACE1) in complex with OM99-2 showed that the bilobal structure of memapsin 2 has the conserved general fold of an aspartic protease (6). The inhibitor is located in the substrate binding cleft between the NH_2 - and COOH -terminal lobes. The active site of memapsin 2 is more open and less hydrophobic than that of other human aspartic proteases. The subsite locations from S4 to S2' are well defined, providing a template for rational drug design against BACE1.

The BACE1 proteins were further characterized by interaction of OM99-2 with both unprocessed and fully processed proteins. Figures 7A and 7B display overlays of the ^{15}N – ^1H NMR HSQC spectra between ligand-free and ligand-

bound states for preproBACE1 and AutoBACE1 proteins, respectively. NMR titration experiments were performed to determine the peak positions of BACE1 in complex with the inhibitor. The intensity changes were followed after each addition of the inhibitor. This allowed the determination of the new peak positions in the presence of the inhibitor. Upon ligand binding, both proteins experienced substantial chemical shift perturbations for many peaks that involve residues in the active site and the flap regions. These residues are in good accordance with the crystallographic data which describe the interaction between inhibitor OM99-2 and BACE1 (6). Interestingly, the overlay of the ^{15}N – ^1H NMR HSQC spectra of both proteins in complex with the inhibitor (Figure 7C) reveals that they are almost identical. Thus, the precursor BACE1 protein rapidly adopted the bound conformation in the presence of the inhibitor, which is identical to the bound conformation for the mature protein. These observations are consistent with the study of the interaction of pro-memapsin 2 and Leu28p-memapsin 2 with OM99-2, which indicated that, once bound, the two enzyme–inhibitor complexes were alike (7). In addition, the interaction of OM99-2 with both preproBACE1 and AutoBACE1 is in slow exchange on the NMR time scale, indicating a strong binding, which is in good agreement with the low nM binding constants of OM99-2 to the two forms of the protein (7). The results of inhibitor binding are consistent with the observation that the active site conformation was conserved during autocatalytic conversion from preproBACE1 to AutoBACE1. Because preproBACE1 has the same active site conformation as the AutoBACE1, it has the same ability to interact with the inhibitor. It also suggests that the pre and pro peptides do not block the active site to hinder the interaction with the inhibitor. A similar result reported that proBACE1 displayed substantial activity relative to mature BACE1 for polypeptide substrate, suggesting that the pro domain has little effect on the BACE1 active site (16).

CONCLUSION

We presented an alternative mechanism for BACE1 conversion, the autocatalytic conversion of preproBACE1. Our study provides further insight into the molecular

mechanisms for the conversion of precursor BACE1 to active proteolytic enzyme. The assigned chemical shifts of AutoBACE1 have been used as probes of structural changes during autocatalytic conversion. The peak distribution in the ^{15}N – ^1H HSQC spectra of the unprocessed preproBACE1 is typical for a partially disordered protein, and that of the fully processed AutoBACE1 represents a well-folded conformation. Analysis of chemical shift changes accompanying the conversion revealed local conformational changes that are spatially concentrated in the NH_2 -terminal lobe. However, the active site conformations are well conserved in both unprocessed and fully processed BACE1. The binding activity was tested by interaction with a substrate-based transition state BACE1 peptide inhibitor. PreproBACE1 rapidly adopted the bound conformation in the presence of the inhibitor, which is identical to the bound conformation for the mature protein. NMR data demonstrated that the pro domain does not significantly hinder inhibitor binding and may assist in the proper folding of the protein. The fully processed AutoBACE1 represents a high quality well-folded protein which is highly stable over long periods of time, and is suitable for evaluation of inhibitor binding by NMR and for NMR-based screening for drug intervention (23).

ACKNOWLEDGMENT

We thank Dr. Charles McNemar for N-terminal sequencing of BACE1 and Dr. Yan-Hui Liu for LS–MS measurements. We also thank Dr. Birendra Pramanik for discussion of the manuscript.

REFERENCES

- Buxbaum, J. D., Liu, K.-N., Luo, Y., Slack, J. L., Stocking, K. L., Peschon, J. J., Johnson, R. S., Castner, B. J., Cerretti, D. P., and Black, R. A. (1998) Evidence that tumor necrosis factor α converting enzyme is involved in regulated α -secretase cleavage of the Alzheimer amyloid protein precursor, *J. Biol. Chem.* **273**, 27765–27767.
- Vassar, R. (2004) BACE1: The β -secretase enzyme in Alzheimer's disease, *J. Mol. Neurosci.* **23**, 105–113.
- Wolfe, M. S., Xia, W., Ostaszewski, B. L., Diehl, T. S., Kimberly, W. T., and Selkoe, D. J. (1999) Two transmembrane aspartates in presenilin-1 required for presenilin endoproteolysis and γ -secretase activity, *Nature* **398**, 513–517.
- Vassar, R. (2002) β -secretase (BACE) as a drug target for Alzheimer's disease, *Adv. Drug Delivery Rev.* **54**, 1589–1602.
- Vassar, R., Bennett, B. D., Babu-Khan, S., Kahn, S., Mendiaz, E. A., Denis, P., Teplow, D. B., Ross, S., Amarante, P., Loeloff, R., Luo, Y., Fisher, S., Fuller, J., Edenson, S., Lile, J., Jarosinski, M. A., Biere, A. L., Curran, E., Burgess, T., Louis, J. C., Collins, F., Treanor, J., Rogers, G., and Citron, M. (1999) Beta-secretase cleavage of Alzheimer's amyloid precursor protein by the transmembrane aspartic protease BACE, *Science* **286**, 735–741.
- Hong, L., Koelsh, G., Lin, X., Wu, S., Terzyan, S., Ghosh, A. K., Zhang, X. C., and Tang, J. (2000) Structure of the protease domain of memapsin 2 (β -secretase) complexed with inhibitor, *Science* **290**, 150–153.
- Ermoliev, J., Loy, J. A., Koelsh, G., and Tang, J. (2000) Proteolytic activation of recombinant pro-memapsin 2 (pro- β -secretase) studied with new fluorogenic substrates, *Biochemistry* **39**, 12450–12456.
- Hong, L., and Tang, J. (2004) Flap position of free memapsin 2 (β -secretase), a model for flap opening in aspartic protease catalysis, *Biochemistry* **43**, 4689–4695.
- Citron, M. (2004) β -secretase inhibition for the treatment of Alzheimer's disease—promise and challenge, *Trends Pharmacol. Sci.* **25**, 92–97.
- Coburn, C. A., Stachel, S. J., Li, Y.-M., Rush, D. M., Steele, T. G., Chen-Dodson, E., Holloway, M. K., Xu, M., Huang, Q., Lai, M.-T., DiMuzio, J., Crouthamel, M.-C., Shi, X.-P., Sardana, V., Chen, Z., Munshi, S., Kuo, L., Makara, G. M., Annis, D. A., Tadikonda, P. K., Nash, H. M., Vacca, J. P., and Wang, T. (2004) Identification of a small molecule nonpeptide active site β -secretase inhibitor that displays a nontraditional binding mode for aspartyl proteases, *J. Med. Chem.* **47**, 6117–6119.
- Cumming, J. N., Iserloh, U., and Kennedy, M. E. (2004) Design and development of BACE-1 inhibitors, *Curr. Opin. Drug Discovery Dev.* **7**, 536–556.
- John, V., Beck, J. P., Bienkowski, M. J., Sinha, S., and Heinrikson, R. L. (2003) Human β -secretase (BACE) and BACE inhibitors, *J. Med. Chem.* **46**, 4625–4630.
- Khan, A. R., and James, M. N. G. (1998) Molecular mechanisms for the conversion of zymogens to active proteolytic enzymes, *Protein Sci.* **7**, 815–836.
- Baker, D., Shiau, A. K., and Agard, D. A. (1993) The role of pro regions in protein folding, *Curr. Opin. Cell Biol.* **5**, 966–970.
- Yan, R., Bienkowski, M. J., Shuck, M. E., Miao, H., Tory, M. C., Pauley, A. M., Brashler, J. R., Stratman, N. C., Mathews, W. R., Buhl, A. E., Carter, D. B., Tomasselli, A. G., Parodi, L. A., Heinrikson, R. L., and Gurney, M. E. (1999) Membrane-anchored aspartyl protease with Alzheimer's disease β -secretase activity, *Nature* **402**, 533–537.
- Shi, X.-P., Chen, E., Yin, K.-C., Na, S., Garsky, V. M., Lai, M.-T., Li, Y.-M., Platchek, M., Register, R. B., Sardana, M. K., Tang, M.-J., Thiebeau, J., Wood, T., Shafer, J. A., and Gardell, S. J. (2001) The pro domain of β -secretase does not confer strict zymogen-like properties but does assist proper folding of the protease domain, *J. Biol. Chem.* **276**, 10366–10373.
- Mori S., Abeysunawardana C., Johnson M. O., Berg, J., and van Zijl P. C. (1995) Improved sensitivity of HSQC spectra of exchanging protons at short interscan delays using a new fast HSQC (FHSQC) detection scheme that avoids water saturation, *J. Magn. Reson., Ser B* **108**, 94–98.
- Kennedy, M. E., Wang, W., Song, L., Lee, J., Zhang, L., Wong, G., Wang, L., and Parker, E. (2003) Measuring human β -secretase (BACE1) activity using homogeneous time-resolved fluorescence, *Anal. Biochem.* **319**, 49–55.
- Sinha, S., Anderson, J. P., Barbour, R., Basi, G. S., Caccavello, R., Davis, D., Doan, M., Dovey, H. F., Frigon, M., Hong, J., Jacobson-Croak, K., Jewett, N., Keim, P., Knops, J., Lieberburg, I., Power, M., Tan, H., Tatsuno, G., Tung, J., Schenk, D., Seubert, P., Suomensaari, S. M., Wang, S., Walker, D., Zhao, J., McConlogue, L., and John, V. (1999) Purification and cloning of amyloid precursor protein β -secretase from human brain, *Nature* **402**, 537–540.
- Christodoulou, J., Larsson, G., Fucini, P., Connell, S. R., Pertinhez, T. A., Hanson, C. L., Redfield, C., Nierhaus, K. H., Robinson, C. V., Schleucher, J., and Dobson, C. M. (2004) Heteronuclear NMR investigations of dynamic regions of intact *Escherichia Coli* ribosomes, *Proc. Natl. Acad. Sci. U.S.A.* **101**, 10949–10954.
- Liu, D., Wang, Y.-S., Gesell, J. J., Wilson, E., Beyers, B. M., and Wyss, D. F. (2004) Letter to the Editor: Backbone resonance assignments of the 45.3 kDa catalytic domain of human BACE1, *J. Biomol. NMR* **29**, 425–426.
- Evenas, J., Tugarinov, V., Skrynnikov, N. R., Goto, N. K., Muhandiram, R., and Kay, L. E. (2001) Ligand-induced structural changes to maltodextrin-binding protein as studied by solution NMR spectroscopy, *J. Mol. Biol.* **309**, 961–974.
- Gesell, J. J., McCoy, M. A., Senior, M. M., Wang, Y.-S., and Wyss, D. F. (2005) NMR-based screening applied to drug discovery targets, *Handbook of Modern Magnetic Resonance*, in press.

BI0510400